ACS OMEGA

Article

Cite This: ACS Omega 2018, 3, 5771−5782

Does the Processing Method Resulting in Different States of an Interconnected Network of Multiwalled Carbon Nanotubes in Polymeric Blend Nanocomposites Affect EMI Shielding Properties?

Shital Patangrao Pawar,[†,§] Piotr Rzeczkowski,[‡] Petra Pötschke,[*,‡] Beate Krause,[‡] and Suryasarathi Bose[*,†]

[†]Department of Materials Engineering, Indian Institute of Science, Bangalore 560012, India

[‡]Department of Functional Nanocomposites and Blends, Leibniz Institute of Polymer Research Dresden, Hohe Str. 6, D-01069 Dresden, Germany

Supporting Information

ABSTRACT: Electromagnetic interference (EMI), an unwanted phenomenon, often affects the reliability of precise electronic circuitry. To prevent this, an effective shielding is prerequisite to protect the electronic devices. In this study, an attempt was made to understand how processing of polymeric blend nanocomposites involving multiwalled carbon nanotubes (MWCNTs) affects the evolving interconnected network structure of MWCNTs and eventually their EMI shielding properties. Thereby, the overall blend morphology and especially the connectivity of the polycarbonate (PC) component, in which the MWCNTs tend to migrate, as well as the perfectness of their migration, and the state of nanotube dispersion are considered. For this purpose, blends of varying composition of PC and poly(methyl methacrylate) were chosen as a model system as they show a phase diagram with lower critical solution temperature type of characteristic. Such blends were processed in two different ways: solution mixing (from the homogeneous state) and melt mixing (in the biphasic state). In both the processes, MWCNTs (3 wt %) were mixed into the blends, and the evolved structures (after phase separation induced by annealing in solution-mixed blends) and the quenched structures (as the blends exit the extruder) were systematically studied using transmission electron microscopy (TEM). Both the set of blends were subjected to the same thermal history, however, under different conditions such as under quiescent conditions (in the case of solution mixing) and under shear (in the case of melt mixing). The electrical volume conductivity and the evolved morphologies of these blend nanocomposites were evaluated and correlated with the measured EMI shielding behavior. The results indicated that irrespective of the type of processing, the MWCNTs localized in the PC component; driven by thermodynamic factors and depending on the blend composition, sea-island, cocontinuous, and phase-inverted structures evolved. Interestingly, the better interconnected network structures of MWCNTs observed using TEM in the solution-mixed samples together with larger nanotube lengths resulted in higher EMI shielding properties (−27 dB at 18 GHz) even if slightly higher electrical volume conductivities were observed in melt-mixed samples. Moreover, the shielding was absorption-driven, facilitated by the dense network of MWCNTs in the PC component of the blends, at any given concentration of nanotubes. Taken together, this study highlights the effects of different blend nanocomposite preparation methods (solution and melt) and the developed morphology and nanotube network structure in MWCNT filled blend nanocomposites on the EMI shielding behavior.

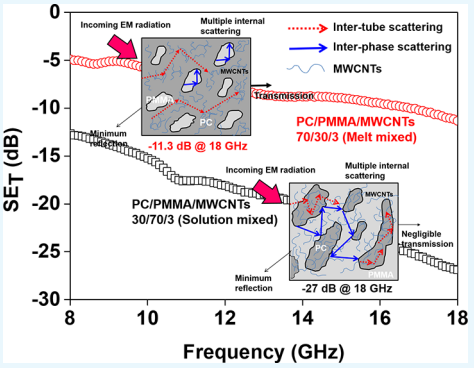

1. INTRODUCTION

Electromagnetic radiation impacts almost all electronic and electrical devices, which can lead to their improper operating conditions or in some cases even to their damage. Electromagnetic interference (EMI) problems can occur in any range of electromagnetic waves, but most of them are caused by radio and microwave frequencies between 100 kHz and few gigahertz. Therefore, an effective EMI shielding, which could minimize or even prevent the impact of electromagnetic radiation, is desirable in every electronic and electrical device.[1]

For an effective shielding, materials with high electrical conductivity or high magnetic permeability are needed. Metals and some polymer composites filled with conductive fillers were explored as suitable materials for shielding because of their good electrical properties, although the mechanism of shielding in metals and conducting particle filled polymers can be very different. EMI shielding is based on three mechanisms, that is, the electromagnetic wave can be either reflected from the outer surface of the shield or absorbed within the shielding material

Received: March 26, 2018
Accepted: May 16, 2018
Published: May 29, 2018

DOI: 10.1021/acsomega.8b00575
ACS Omega 2018, 3, 5771−5782

or can be reflected from the internal surfaces of the shield inducing multiple reflections.[1]

In designing of an enclosure/housing for shielding applications, one of the most important concerns is the weight as the current electronic era has drifted toward miniaturization. Therefore, lightweight and noncorrosive polymeric materials with conducting fillers offer huge advantage over other conductive materials such as metals which are heavier.[2] Owing to their exceptional properties, polymer nanocomposites containing carbon nanotubes (CNTs) have been developed for various applications.[3−5] Recent review articles highlight the key role of polymeric nanocomposites especially containing carbonaceous fillers for EMI shielding applications.[2,6,7] Among the various allotropes of carbon, CNTs are considered as one of the best conductive nanofillers because of their high inherent electrical conductivity, high mechanical properties, and high aspect ratio, thereby providing sufficient electrical conductivity to composites at relatively lower concentration[8] as compared to conventional fillers such as carbon black. Significant improvement in electric properties and EMI shielding is observed with CNT concentration reaching or exceeding the electrical percolation threshold.[2] In ref 9, it was proposed that microwave absorption can be optimized by adding a certain amount of CNTs slightly above the percolation threshold and that the broadband absorption can be improved by designing multilayered structures. It has been well-established that the microwave absorption in polymer-based nanocomposites can be enhanced through uniquely structured nanocomposites such as layer-by-layer assembly,[10−12] multilayered structure,[13] and foamed structures.[14−17] The thermal annealing of polymer nanocomposites also depicted significant effect on EM absorption.[18] Moreover, interconnected networks of conducting nanoparticles in a given polymer matrix facilitate the elimination of incoming microwave radiation.[19] Therefore, large efforts have been involved in enhancing the dispersion quality of nanoparticles in polymer matrices through covalent and noncovalent attachment of functional moieties on the surface of conducting nanoparticles,[20−22] anchoring hybrid fillers such as metals and ceramic particles to the surface of conducting nanoparticles,[23−25] and incorporating secondary fillers.[26] In this context, processing methodology employed for the preparation of nanocomposites also plays a vital role in dispersion and network formation of nanoparticles in a given matrix and thereby on the final EMI shielding performance of the nanocomposites.

In this context, preparing conducting polymer nanocomposites involving CNTs requires that the nanotubes are well-individualized but at the same time form an interconnected network-like structure in the matrix. However, most often, even if a well-dispersed state is generated, depending on various effects during fabrication processing, such as crystallization, curing, viscosity changes, and so forth, the final state of dispersion of CNTs can be negatively affected, resulting in lower electrical conductivity than theoretically expected. Alternatively, a strategy to facilitate an interconnected network-like structure of CNTs in a matrix at low loadings is to localize them in a given component of a cocontinuous blend.[27−30] To this end, several reports have been published as to how CNTs migrate to their preferred component in binary blends either during processing or postprocessing operations such as annealing, injection molding, and so forth.[28,31,32] Interesting observations were reported especially with partially miscible systems such as poly(α-methyl styrene-*co*-acrylonitrile)/poly(methyl methacrylate) (PMMA), polystyrene/poly(vinyl methyl ether), and PMMA/styrene-acrylonitrile (SAN) to name a few. It is worth noting that CNTs are randomly distributed in these homogeneous blends and migrate to the preferred component during demixing. This, besides altering the overall charge transport in the blends, also influences the evolving morphology during demixing. Recently, immiscible blends with cocontinuous phase morphology illustrated a positive impact on EMI shielding performance.[6,30] Though immiscible blends have been widely studied, the effect of phase separation [as in polycarbonate (PC)/PMMA] is not yet fully understood, especially concerning EMI shielding. Therefore, among the different pairs of partially miscible blends, we focused on a particular pair: PC and PMMA, which shows a cocontinuous type of morphology in a fixed compositional window.[33−37] In the case of PC/PMMA blends, the effect of the processing technique on the miscibility of phases is well-established where melt mixing leads to phase-separated blends and solution mixing provides homogeneous mixtures.[38] However, in the case of solution-mixed blends, miscibility is due to kinetically trapped polymer components in the homogeneous state below the glass-transition temperature (T_g). In this case, phase separation is often realized by heating the blend above the T_g, which is mainly due to very slow separation from the nonequilibrium miscible state.[39] Certain literature reported that higher amount of PMMA (ca. 90 wt %) or PC (ca. 70 wt %) results in phase-inverted structures. Besides composition, the viscosity ratio also plays a major role in yielding this transient morphology. It has been reported[37] that for PC/PMMA blends with 50−70 wt % of PMMA with lower viscosity PC or 60−70 wt % of PMMA with higher viscosity PC, a cocontinuous morphology could be observed.

Although PC/PMMA blends exhibit partial miscibility under certain conditions, they phase-separate into different microstructures upon annealing. Under the light of the existing literature, it is evident that by adding nanoparticles, the various transient morphologies can be stabilized—an action very similar to the classical block copolymer route but with a different mechanism. Depending on the polarity and the surface wetting, CNTs often localize in a component with higher polarity, thereby minimizing the interfacial tension between the component and CNTs. Among the different blend systems studied involving PC, it is observed that CNTs mostly localize in the PC component possibly driven by their higher polarity and/or lower melt viscosity.[35,36,40] In ref 36, it was proposed, based on interfacial energy calculations using geometric and harmonic mean equations, that the CNTs migrated and localized in the PC component within a PC/PMMA blend. In blends of PC/SAN,[35,40] the CNTs mostly localized in the PC component, and by precompounding SAN with a reactive maleic anhydride group, the localization of CNTs in the SAN component was induced against the thermodynamic factors, which is responsible for the localization of CNTs in the PC component in the blends.[40]

Under this framework, it is evident that migration and localization of CNTs in a bicomponent system besides controlling the blend morphology also influence the overall interconnected network structure of nanotubes in the blends. As migration through viscous polymer melts is relatively slower, the formation of interconnected network-like structures of CNTs is impeded and often difficult to reach equilibrium within the processing timeframe. This study mainly compares between different processing (melt vs solution mixing)

DOI: 10.1021/acsomega.8b00575
ACS Omega 2018, 3, 5771−5782

methods toward the overall conducting network of MWCNTs in a partially miscible system (PC/PMMA). Besides, this work also focuses on developing lightweight EMI shielding enclosures utilizing the interconnected network-like structure of MWCNTs in various PC/PMMA blends processed in the two different ways. Following the selective localization of MWCNTs during processing or postprocessing operations in a given component, a conductive pathway is developed in the blends. These conducting blends were then evaluated for EMI shielding applications. A detailed transmission electron microscopic (TEM) analysis was carried out to understand the migration and localization of MWCNTs in the blends. The DC electrical conductivity was measured to obtain the volume resistivity/conductivity of various blend systems. Finally, the different blend nanocomposites were evaluated for EMI shielding properties, and the mechanism of shielding was systematically studied. Taken together, this study makes an attempt to understand as to how processing different conducting blend nanocomposites alters the overall state of dispersion of MWCNTs and how the final quality of dispersion affects the EMI shielding properties. This study will help guide researchers working in this area from both fundamental and end-application point of view.

2. RESULTS AND DISCUSSION

2.1. Evolution of Morphology during Processing and Postprocessing of PC/PMMA Blends with MWCNTs. The morphology of the solution- and melt-mixed blend nanocomposites was evaluated systematically using TEM to gain an insight on two different aspects. First, the distribution of components in the blends and second, the localization and the quality of dispersion of MWCNTs in the blend nanocomposites that were prepared by the two different mixing processes (melt vs solution). As mentioned earlier, the content of MWCNTs was varied from 1 to 3 wt % in various PC/PMMA blends (30/70, 50/50, 60/40, and 70/30 by weight); however, for TEM analysis, only blends with 3 wt % MWCNTs were chosen to gain an insight in the process-induced changes on the overall state of dispersion of MWCNTs. First, micrographs with lower magnifications were captured to illustrate the distribution of the components (PC and PMMA) in the blend nanocomposites. The images with higher magnification were further recorded to reveal the localization and the state of dispersion of MWCNTs in the blends. An important difference between the morphology of the melt-mixed and solution-processed blends is worth noting at this point. For effective comparison of solution-processed and melt-mixed samples, representative samples were melt-extruded under different processing conditions, and the resulting volume conductivity was evaluated (not shown here). On the basis of these results, the optimized processing parameters obtained were 260 °C for 20 min at 60 rpm screw speed. The TEM micrographs of melt-mixed samples represent the evolved structures after the extrusion process (260 °C for 20 min, where the blends are already phase-separated). As the melt leaves the die, the morphology is quenched and thin sections were ultramicrotomed from the extruded solid strands without any further treatment. In contrast, the TEM micrographs of solution-processed samples (from the homogeneous state) were obtained after hot-pressing them in a lab-scale compression molding machine at 260 °C for 20 min to induce phase separation. Although both the set of blends were subjected to 20 min at 260 °C, the nature of processing the blend nanocomposites widely varies. In the first case (melt mixing), the blends are sheared at high temperature where de-entanglement of MWCNTs is expected. In the second case (solution processing), though the quality of dispersion of MWCNTs is expected to be better because of lower solution viscosities compared to higher melt viscosities, during annealing (hot-pressing), the MWCNTs migrate to their preferred phase, while the blends phase-separate into PC-rich and PMMA-rich phases. This leaves less time for the MWCNTs to develop fully interconnected network-like structures in contrast to melt-mixed samples. The as-prepared solution-mixed samples (before compression molding) showed single glass-transition temperatures (see Figure S1), further confirming the homogeneous state of the samples. It is only during compression molding that the blends phase-separate as the temperature is much above the glass-transition temperature of both the components (see Figure S1). It is well-understood that the blend components are kinetically arrested when heated above the glass-transition temperature. Hence, the effective aspect ratio of MWCNTs is expected to be higher in solution-mixed blends when compared with melt-processed samples (where high shear stresses may break nanotubes and reduce the effective aspect ratio). As PC/PMMA blends exhibit lower critical solution temperature (LCST) type of behavior (above the glass-transition temperatures of the components), we expect two phenomena to occur during compression molding: first, the development of the blend microstructure and second, the migration/selective localization of the nanotubes to the preferred component (here PC). The objective of the following section is to take a closer look at the various morphologies during processing or postprocessing operation in the case of blend nanocomposites. This section is important from a fundamental point of view as the overall state of dispersion and localization of MWCNTs will greatly influence the conductivity and the EMI shielding properties.

2.2. TEM of Melt-Mixed Samples. Figure 1 presents the TEM images of melt-mixed PC/PMMA 30/70 w/w % blends

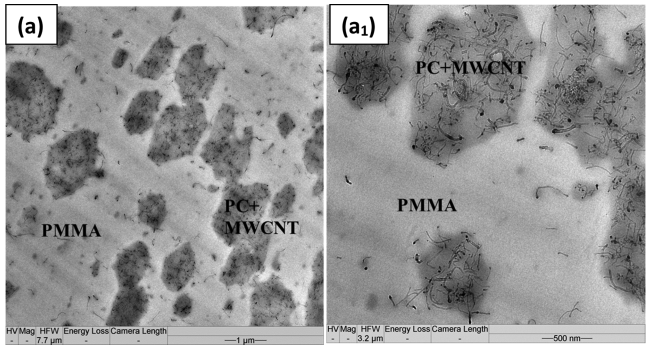

Figure 1. TEM micrographs of PC/PMMA 30/70 blends containing 3 wt % MWCNTs prepared by melt mixing: (a) low magnification and (a_1) high magnification.

containing 3 wt % MWCNTs. The darker regions in the captured micrographs represent the PC component because of preferential interaction with the electron beam, and the lighter regions can be assigned to the PMMA component, which tends to be less affected by the electron beam. It is evident that the PC component is dispersed in the PMMA matrix; however, the morphology is strikingly different than the typical matrix-droplet morphology (where often spherical droplets are dispersed in a matrix). Another interesting feature worth

DOI: 10.1021/acsomega.8b00575
ACS Omega 2018, 3, 5771−5782

mentioning is that the MWCNTs are localized in the PC component of the blend and also observed to bridge the components. This observation has been reported before in the literature where high aspect ratio fillers (such as CNTs) especially bridge the domains in cases where their characteristic lengths are larger than the domain sizes.[41−43] In addition, the preferred presence of MWCNTs in a given component in biphasic systems often slows down the relaxation of that particular phase and thereby prevents it from further coarsening. This phenomenon typically results in irregular structures in filled blends. A recent perspective article elaborates this phenomenon in greater detail.[44] As the MWCNTs are localized in the minor component (here PC), the effective concentration of the nanotubes in that particular component increases significantly, resulting in a dense network-like structure of nanotubes as clearly observed in Figure 1. This also agrees with experimental results reported earlier in refs,[36,40,45] where CNTs tend to localize in the PC component within a blend structure consisting of PC/PMMA[45] or PC/SAN.[36,40]

Figure 2 presents the TEM micrographs of melt-mixed PC/PMMA 50/50 blends with 3 wt % MWCNTs. The morphology

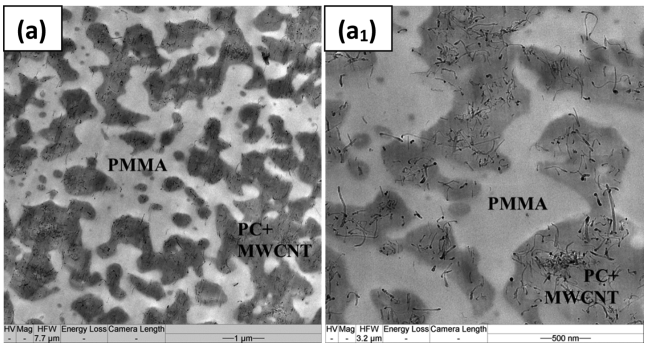

Figure 2. TEM micrographs of PC/PMMA 50/50 blends containing 3 wt % MWCNTs prepared by melt mixing: (a) low magnification and (a_1) high magnification.

observed in the thin two-dimensional cuts suggests that both the components are continuous (with few isolated domains of the PC component) and that MWCNTs are localized in the PC component. The MWCNTs in the PC component are well-dispersed and form an interconnected network-like structure. Unlike the 30/70 blends, the 50/50 blends showed relatively better dispersion of nanotubes as the volume available for the dispersion of the nanotubes is ca. 1.7 times larger. Similar to 50/50 PC/PMMA blends, the 60/40 PC/PMMA blends with MWCNTs also show cocontinuous type of morphology (see Figure 3a). In this case, the interconnected PC domains are more evident as compared to the 50/50 composition. The MWCNTs are nicely localized in the PC component with relatively good dispersion. The shearing action during extrusion facilitates the dispersion process of primary MWCNT agglomerates which were infiltrated by the polymer melt. There is a trade-off between higher shear stresses, resulting in better dispersion and nanotube length shortening during the melt-extrusion process.[46−50] The higher the shear, the more is the shortening of the nanotubes,[47,49,51] which often is not desired for designing conducting blend nanocomposites. To understand this trade-off, as mentioned earlier, based on the conductivity results of the samples processed at different processing conditions, the optimized processing parameters

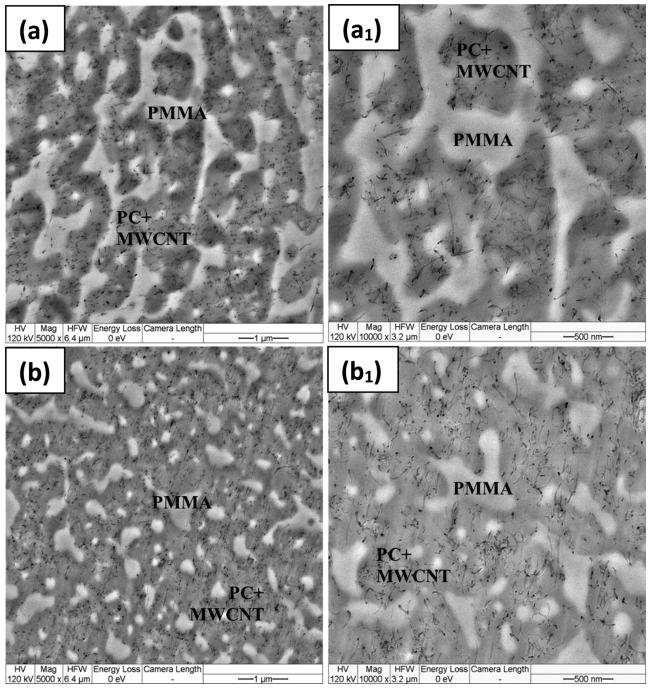

Figure 3. TEM micrographs of PC/PMMA (a) 60/40 and (b) 70/30 blends containing 3 wt % MWCNTs prepared by melt mixing. (a_1) and (b_1) are high-resolution images of the respective blend nanocomposites.

obtained were 260 °C for 20 min at 60 rpm screw speed (not shown here). The observed cocontinuous morphology is also in agreement with other reports presenting cocontinuous structures with 50 wt %[34,35] and with 47 wt % of PMMA[33] in PC.

Figure 3b presents the TEM micrographs of PC/PMMA 70/30 blends. A distinct phase inversion was observed in this case where PMMA domains are distributed in PC. Unlike 30/70 blends, in this case much smaller PMMA domains with sizes of 200−500 nm are well-dispersed in the PC matrix. This observation is related to slowing down of the relaxation of the filled component thereby suppressing the coarsening phenomenon, as it was discussed earlier. In the case of 70/30 PC/PMMA blends, because the droplets of the PMMA component are free of nanotubes, they can easily form a regular droplet shape with fewer coalesced droplets. As the surrounding matrix is expected to be of higher viscosity because of the presence of nanotubes, the droplet deformation is expected to be higher during processing. Hence, much smaller droplets appear in the case of 70/30 blends when compared with the 30/70 blends. Taken together, from the TEM analysis, it is evident that irrespective of the composition, the MWCNTs localize in the PC component driven by thermodynamic factors. Further, the quality of dispersion of the nanotubes depends largely on the amount in which it is localized, as this determines the effective filler concentration. If the component which is preferred for the nanotube localization (here PC) is the minor component in the blends, the effective filler concentration becomes significantly higher and results in denser interconnected networks of CNTs as compared to blends with PC as the major component. However, the state of dispersion appears to be better upon localization in the major PC component. Because the connected network of nanofillers in the polymer matrix is crucial for electrical conductivity and

DOI: 10.1021/acsomega.8b00575
ACS Omega 2018, 3, 5771−5782

EMI shielding effectiveness of the blend nanocomposites, the connectivity of the filled component also plays a vital role. It is expected that blends with the continuous PC component, achieved in blends with PC as the matrix, and cocontinuous blends, only reached in a certain blend composition range, are preferred for better properties. At different blend morphology types, the desired multiple scattering between neighbored nanotubes and multiple scattering between conducting domains has a different impact on attenuating the incoming EMI radiation.

2.3. Optical Microscopy (OM) and TEM of Solution-Mixed Samples. PC/PMMA solution-mixed samples were prepared in addition to melt-mixed samples to clearly understand how different blend preparation processes influence the overall state of dispersion and distribution of the nanotubes in blend nanocomposites. The PC/PMMA blends with MWCNTs were obtained from the homogeneous mixing state and later subjected to the compression molding process at 260 °C for 20 min to induce the phase separation. Although both sets of blends were subjected to similar thermal conditions, the evolving structures are expected to be very different for shear (as in the extrusion mixing) and squeeze flow deformation (as in compression molding shaping) processes. As the two techniques of melt mixing and solution mixing followed by compression molding are often used to fabricate nanocomposites and blends, it is worth investigating how the evolved structures and the continuity of the filled component together with the quality of nanotube dispersion affect the electrical conductivity and EMI shielding properties.[52]

Before looking at high-magnification TEM micrographs, optical micrographs of these solution-mixed blends after compression molding were observed to get a general impression about the blend morphology and nanotube agglomerate sizes. As discussed earlier, the solution-mixed samples exhibited a single glass-transition temperature confirming their thermodynamically miscible state (see Figure S1). As the glass-transition temperatures of both the components are far apart, overlapping glass transitions manifesting in a single thermal transition in differential scanning calorimetry (DSC) are ruled out. Because the hot-pressing temperature is well above the LCST temperature of the blend system, during the hot-pressing step at 260 °C for 20 min more or less complete phase separation is expected. The optical micrographs of the as-pressed different blend nanocomposites with 3 wt % MWCNTs are shown in Figure 4. In the images, the phase separation resulting in cocontinuous structures with a bright (CNT-free) component and another one with gray color of different intensities (CNT containing) can be seen together with remaining black CNT agglomerates of different sizes and shapes. This confirms the expectation that at 260 °C, the blends phase-separate into PC-rich and PMMA-rich phases and the nanotubes migrate to the preferred component (here PC). The blends might undergo coarsening but to a limited extent because of the presence of morphology stabilizing MWCNTs. However, as the focus of this work is to understand the process-induced dispersion of MWCNTs and its effect on EMI shielding, the coarsening phenomenon was not studied here and is subjected to future investigations.

Looking in more detail, the TEM micrographs of PC/PMMA blends containing 3 wt % MWCNTs prepared by solution mixing shown in Figure 5 clearly illustrate that the darker regions correspond to the PC component and the lighter regions to PMMA. In 30/70 PC/PMMA blends (see Figure 5a), interestingly, the filled PC component appears to form large interconnected structures in the PMMA matrix, whereas in the 50/50 PC/PMMA blends (see Figure 5b), it seems that both components form larger domains and a more pronounced segregation of the nanotubes in the PC component. The cocontinuous structure is more clearly seen for the 60/40 and 70/30 PC/PMMA blends (Figure 5c,d), whereby the smallest domain sizes and most interconnectivity are seen in the 70/30 blend. As in the case of melt-mixed samples, the localization of MWCNTs in the PC component was consistent in the solution-mixed samples as well; however, the perfectness of migration slightly depends on the general blend composition. If PC forms the minor component (like in the 30/70 blend), it seems to be more difficult for the nanotubes to migrate to PC,

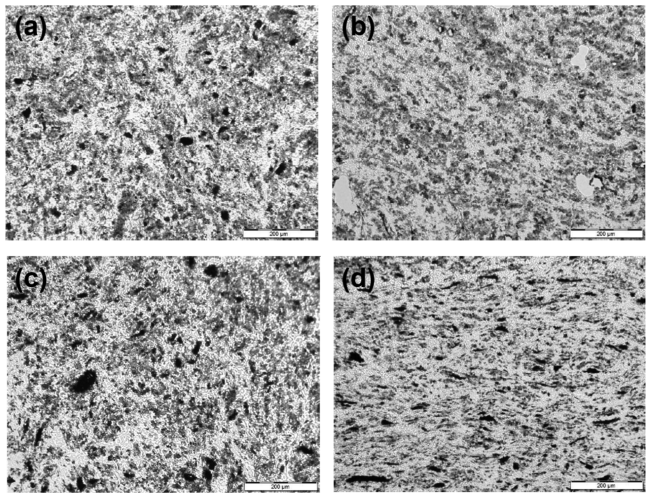

Figure 4. Optical micrographs of solution-mixed PC/PMMA (a) 30/70, (b) 50/50, (c) 60/40, and (d) 70/30 blends containing 3 wt % MWCNTs after compression molding.

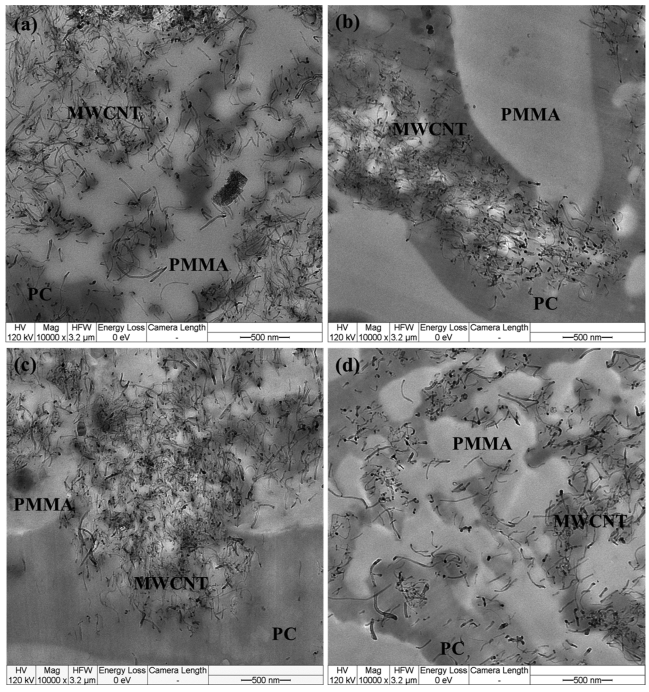

Figure 5. TEM images of solution-mixed and compression-molded polymer PC/PMMA composites containing 3 wt % MWCNTs with weight ratios of (a) 30/70, (b) 50/50, (c) 60/40, and (d) 70/30.

DOI: 10.1021/acsomega.8b00575
ACS Omega 2018, 3, 5771−5782

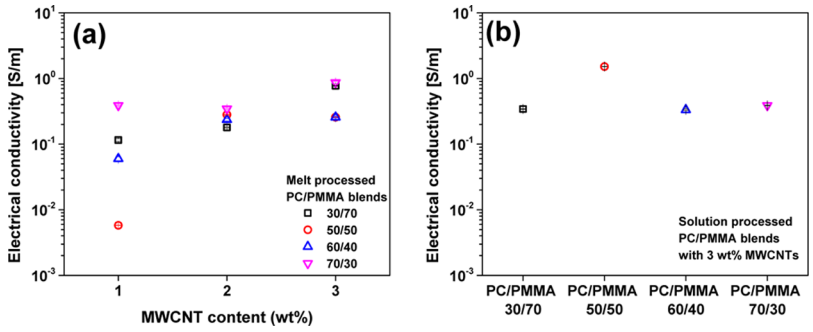

Figure 6. DC volume conductivity of (a) melt-processed PC/PMMA blends as a function of MWCNT content and (b) various solution-processed PC/PMMA blends containing 3 wt % MWCNTs.

whereas in the 70/30 blend, a more perfect localization in PC is observed. This suggests that the general localization of nanotubes within the PC component is the same irrespective of the way the blends are made.

By comparing the TEM micrographs of both sets of blends, it is very evident that the general state of nanotube dispersion and the perfectness of selective localization in the PC component are better in the melt-mixed samples, which also show finer blend morphologies. Thus, it appears that the nanotubes and their more pronounced agglomeration state delay the demixing in the solution-based PC/PMMA blends during compression molding, resulting in more irregular microstructures.

Although the nanotubes undergo intense shearing during the nanocomposite preparation in solution mixing, the efficiency of disentanglement of agglomerates seems to be lower than in melt mixing, resulting in denser interconnected network structures. These structures are rather restricted in migrating to the thermodynamically preferred PC. It is expected that the dispersion of the nanotubes is better in solution-mixed blends because of the ease in penetration of the dissolved polymer chains into the nanotube agglomerates, which reduces their agglomerate strength and helps finally in the agglomerate breakup. However, this could not be confirmed by the TEM images of both blend series. However, it appears that the nanotubes in the TEM images are much shorter in melt-mixed blends as compared to the solution-mixed. This is possibly due to the higher shear stresses applied inside the micro-compounder. Such effects of shortening CNTs in cocontinuous melt-mixed blends were recently reported by Liebscher et al.,[51] wherein shortening of length of CNTs by 25% of the initial length after melt mixing in a similar kind of microcompounder was reported for PC/SAN 60/40 blends with 1 wt % NC7000. As shorter nanotubes are easier to disperse, the observation of better dispersion in melt-mixed blends may be related to this nanotube breakage. Thus, it may be expected that solution-mixed blends have longer nanotubes facilitating the network formation at lower loadings and resulting in higher absolute electrical conductivity. From the EMI shielding perspective, which is the major focus of this work, larger extended nanotube networks, such as that observed in solution processing, may offer higher intertube scattering than well-dispersed structures localized in one of the components of the blends. To understand the phenomena directing EMI shielding, both the blends were systematically studied for their electrical volume conductivity and EMI shielding properties.

2.4. Electrical Volume Conductivity of PC/PMMA Blends. The electrical volume resistivity was measured for melt-mixed nanocomposites of 30/70, 50/50, 60/40, and 70/30 PC/PMMA blends containing 1, 2, and 3 wt % of MWCNTs. For solution mixing, measurements were performed for four sets of blends: 30/70, 50/50, 60/40, and 70/30 PC/PMMA blends containing only 3 wt % of MWCNTs. PC and PMMA are insulating materials with very low electrical conductivity. Figure 6 shows the DC conductivity versus the nanotube content for melt-mixed blends and all values for solution-mixed blends with 3 wt % MWCNTs. It can be clearly seen that already the addition of 1 wt % MWCNTs to the different melt-mixed PC/PMMA blends makes them conductive.

The highest values of electrical conductivity were measured for nanocomposites made of PC/PMMA 70/30 in which the major PC component forms the matrix phase and by such shows the highest connectivity among all blends. Even if the local CNT content (assuming complete selective localization) is the lowest at this blend composition, the very good dispersion, the distinct selective localization, the perfect PC connectivity, and possibly also a comparatively lower nanotube shortening result in the most conductive networks. The conductivity increases for all blends with MWCNT loading whereby the 60/40 blends showed the lowest conductivity values but the highest relative increase with the nanotube amount. The values found for the volume conductivities are in agreement with previous reports on PC/SAN blend nanocomposites, namely, PC/SAN/CNT 59/40/1 wt %[36] and PC/SAN 60/40 containing 0.5 wt %.[40]

The solution-mixed PC/PMMA blends containing 3 wt % MWCNTs (Figure 6b) exhibit electrical conductivities very close to each other in the range of 0.35−0.4 S/m, except for the 50/50 PC/PMMA blend which exhibits a slightly higher conductivity, illustrating a higher degree of connectivity in this blend, which goes along with the coarser blend structure at this composition. Although the electrical volume conductivities are more or less similar in both sets of blends at a given concentration of nanotubes, the EMI shielding behavior can be very different. As discussed before, the blend morphologies including the connectivity of the conductive component PC, the perfectness of localization in this component, and the state of dispersion (and nanotube length) are different in the blends.

2.5. EMI Shielding: Influence of Intertube and Interphase Scattering. The EMI shielding effectiveness of the PC/PMMA blends prepared by the two different techniques of melt and solution mixing, which are primarily used for the preparation of nanocomposites, was assessed over X and K_u-band frequencies, as this frequency range is essential for most of the commercial applications. Because polymer-based nanocomposites manifest absorption-driven shielding,

DOI: 10.1021/acsomega.8b00575
ACS Omega 2018, 3, 5771−5782

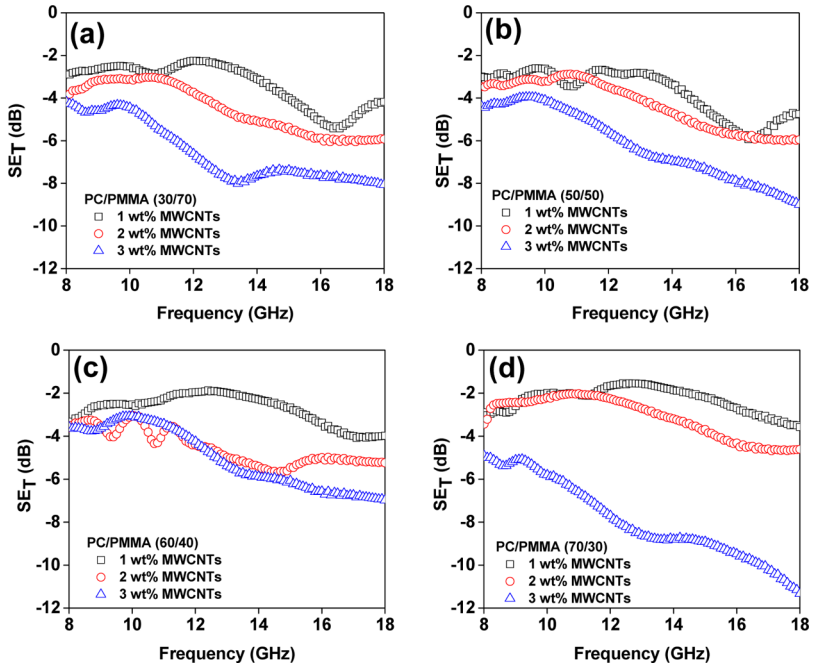

Figure 7. SE_T as a function of frequency for melt-mixed PC/PMMA blends (a) 30/70, (b) 50/50, (c) 60/40, and (d) 70/30 containing different amounts of MWCNTs.

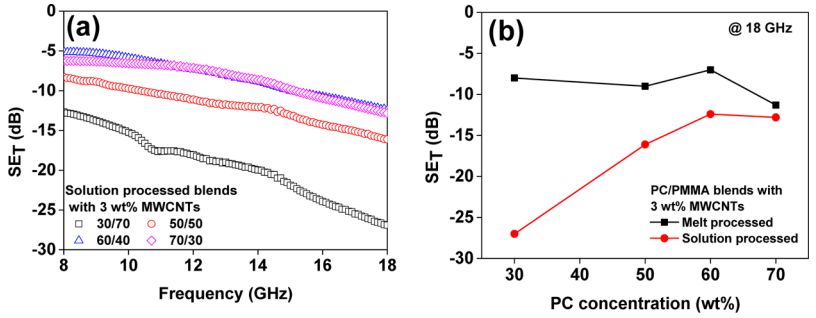

Figure 8. (a) SE_T as a function of frequency for solution-mixed PC/PMMA blends containing 3 wt % MWCNTs and (b) SE_T as a function of PC concentration.

this class of materials has been emerging off late for EMI shielding applications. Recently, owing to their flexibility in developing unique microstructures, phase-separated multiphasic polymer blends resulted in interesting outcomes toward microwave shielding. In this study, different overall blend morphologies and by varying the blend composition, different states of connectivity of the PC component, in which the MWCNTs tend to migrate, as well as different states of perfectness of that migration and of the state of nanotube dispersion were achieved and can be compared.

Figure 7 shows total shielding effectiveness (SE_T) as a function of frequency for melt-processed PC/PMMA blends containing different amounts of MWCNTs. The SE_T scaled with the amount of MWCNTs in the blends and has absolute values as high as the nanotube content. This is mainly attributed to the increased interconnectivity of the nanotube networks of MWCNTs at higher loading and enhanced dielectric loss associated with these denser networks. At higher amount of MWCNTs, the distance between neighboring MWCNTs decreases, resulting in an easier transport of nomadic charges, leading to a larger Ohmic loss. In a recent study, the intertube and especially the interphase scattering was shown to play a vital role in eliminating incoming microwave radiation.[23,24] Intertube scattering corresponds to the scattering of penetrated microwaves from conducting MWCNTs, and interphase scattering represents scattering of penetrated microwaves from the interphase between the different blend components. Thereby, these scattering events are strikingly different from multiple reflections and facilitate the elimination of penetrated microwave radiation. Comparing the different blend compositions, a slight influence of the developed blend microstructure on the SE_T of melt-processed PC/PMMA blends is observed. From TEM analysis, the distinct transition of phase morphologies from the droplet matrix to cocontinuous and finally phase inversion were observed with increasing PC content in the blends. In all the blends, a very pronounced localization of MWCNT in the PC component was found with better states of dispersion at higher PC contents. It has been reported for immiscible polymer blends that at a given concentration of MWCNTs, cocontinuous morphologies lead to enhanced SE_T arising from interconnected MWCNTs and well-connected phases.[30] However, in our study, in the case of melt-mixed blends, the continuous PC matrix filled with MWCNTs and containing finely dispersed PMMA domains

DOI: 10.1021/acsomega.8b00575
ACS Omega 2018, 3, 5771−5782

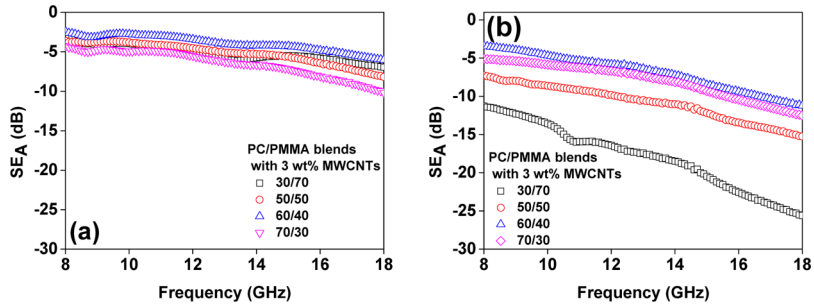

Figure 9. SE_A as a function of frequency for (a) melt-processed and (b) solution-processed PC/PMMA blends containing 3 wt % MWCNTs.

(i.e., 70/30 wt/wt) depicted enhanced SE_T over the other two types of morphologies, which is especially seen at 3 wt % MWCNT loading as shown in Figure 7. In the 70/30 blend, the highest volume of the preferred PC component (as compared to the other blend compositions) is available for the accommodation of the MWCNTs resulting despite a lower local nanotube concentration in a relatively better dispersion of MWCNTs as observed from TEM analysis. In addition, the PC forms a matrix, meaning that a perfect continuous component and the MWCNTs show a high perfectness of migration into that component. This explains why this particular blend shows slightly higher electrical conductivity over the other blend compositions containing 3 wt % MWCNTs. The enhanced SE_T of the 70/30 blend also echoes the same. Therefore, from the detailed TEM analysis (Figures 2 and 3) and EMI shielding performance of melt-mixed blends (Figure 7), one can conclude that the degree of connectivity of the PC component, the perfectness of MWCNT migration into PC, as well as the state of nanotube dispersion govern the final EMI shielding performance of the blends. The better continuous the PC component, the more pronounced the selective localization, and the better the dispersion, the higher the electrical conductivity and EMI shielding efficiency.

The SE_T as a function of frequency for the solution-processed PC/PMMA blends containing 3 wt % MWCNTs is shown in Figure 8a, and the SE_T values of melt- and solution-mixed blends are compared in Figure 8b. It is interesting to note that at the selected concentration of MWCNTs (3 wt %), the effect of blend composition plays a pronounced role. Thereby, the PC/PMMA 30/70 blend has the outstanding highest shielding efficiency followed by 50/50, 70/30, and 60/40 blends, whereas in the melt-mixed blends, the efficiency tended to increase with the higher PC content. Interestingly, all solution-processed blends manifested in remarkably higher absolute values of SE_T than the melt-mixed blends at any given blend composition (Figure 8b). For instance, the best SE_T of −27 dB (@18 GHz), suggesting more than 99% elimination of incoming microwave radiation, was observed for the solution-mixed 30/70 PC/PMMA blend with 3 wt % MWCNTs. Moreover, the observed SE_T value is well above the required threshold for major commercial applications (i.e., ≥−20 dB; absolute value). As depicted in Figure 5, the solution-processed blends, next to differences in the blend morphology when compared with the melt-mixed ones, showed less pronounced perfectness of selective migration of larger nanotube networks into the PC component. Thus, much larger networks span over both components (see Figure 5). In addition, the nanotubes appeared to be longer than in the melt-mixed blends, resulting in an easier network formation at a given loading. The outstanding sample of PC/PMMA 30/70 should have the highest effective concentration of MWCNTs and also shows the lowest perfectness of MWCNT migration into PC. Obviously, a suitable CNT network morphology and spatial arrangement within the blend morphology are formed, which results in the best shielding performance. This sample is followed by the PC/PMMA 50/50 blend, which showed larger blend domains and in context with this more pronounced selective nanotube localization in PC. Thus, a relatively large segregated network spans over the whole blend.

It is important to mention that in contrast to melt-mixed blends, in which conductivity showed a stronger dependence on composition and EMI shielding followed conductivity, in solution-processed blends, the electrical conductivity values of blends did not change much; however, the EMI shielding performance changed drastically. This can be attributed to enhanced intertube scattering because of networks with locally higher density and a large continuous interface generated because of cocontinuous phase morphology. This obviously leads to maximum blocking of penetrated microwave radiation. At higher filler concentration, apart from electrical conductivity, the developed microstructures and interconnections between microwave active particles govern the EMI shielding performance of the blends. Taken together, the synergy between the cocontinuous phase morphology, the better retained nanotube length, and the less perfect selective migration into one component resulted in a type of segregated nanotube network structure generating maximum attenuation of incoming microwave radiation. The results imply that the blend morphology serves as a template for the segregated nanotube network structure, which is in the case of solution-mixed blends less matched as larger network areas than the domain sizes are built. This discrepancy seems to be the highest at low PC content resulting together with the blend interface to the best shielding efficiency of these nanotube networks.

Because the EM smog has become a great threat for safe functioning of precise electronic devices, the attenuation of microwave radiation through absorption is the most desired mechanism. Therefore, in order to study the wave absorption ability of developed blends, shielding effectiveness through absorption (SE_A) of blends was assessed over X and K_u-band frequency range. Figure 9 shows variation in the SE_A for both blend series at different blend compositions. It is seen that irrespective of blend preparation technique and blend composition, all blends manifest absorption-driven microwave shielding. All PC/PMMA blends, irrespective of a processing technique, showed a phase-separated structure with selective localization of MWCNTs in the PC component leaving the PMMA component almost free of nanotubes and thus insulative. Therefore, a large fraction of incoming microwave radiation gets penetrated in the blends (i.e., minimized surface

DOI: 10.1021/acsomega.8b00575
ACS Omega 2018, 3, 5771−5782

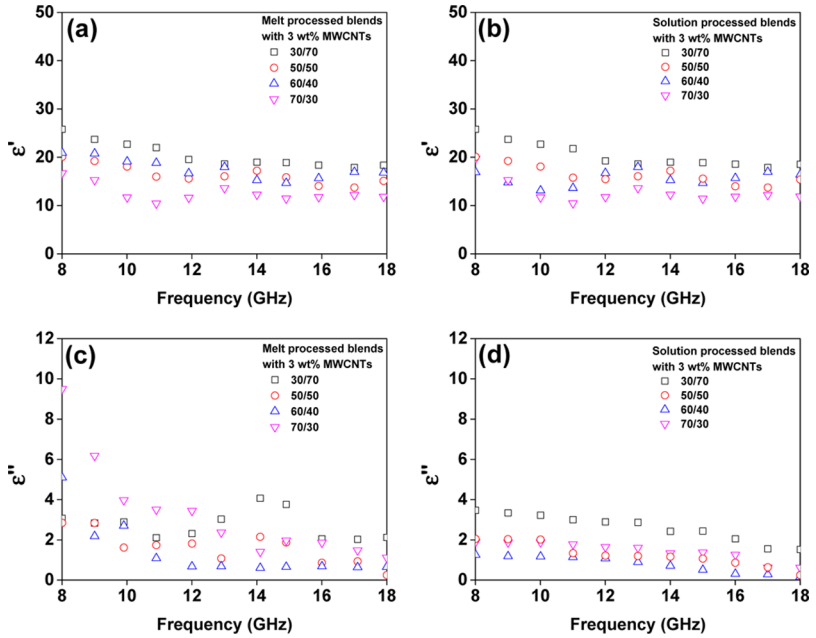

Figure 10. Real permittivity of (a) melt- and (b) solution-processed; imaginary permittivity of (c) melt- and (d) solution-processed PC/PMMA blends containing 3 wt % MWCNTs.

reflection which is essential for microwave-absorbing materials) through the insulative PMMA component, which is further attenuated by interaction with the conducting PC component and the MWCNTs. Hence, the developed blends are not only effective in blocking microwave radiation but also help in controlling EM smog. Interestingly, at a given composition, solution-processed blends showed remarkably higher SE_A over melt-processed (Figure 9). For instance, the solution-mixed PC/PMMA 30/70 blend with cocontinuous morphology depicted the highest absorption of penetrated microwave radiation. Because the electrical conductivity of solution-processed blends, irrespective of composition, was approximately similar, the enhanced SE_A is ascribed to the intertube and interphase scattering in the blends. The effect of blend morphology and dispersion of MWCNTs on microwave absorption ability of blends is well-evident. In the case of polymer-based nanocomposite containing heterogeneous materials with different electrical properties, the scattering of penetrated microwave radiation due to impedance mismatch on the micron length becomes more likely. Each scattering event leads to the decreased power of penetrated microwave radiation and eventually leads to elimination. This is often considered as absorption of microwave radiation through the large dielectric and/or magnetic loss depending on the nature of microwave active fillers. In this case, the multiple scattering events are facilitated by the continuous conducting polymer component (i.e., PC) and interconnected networks of MWCNTs. However, in both the blends prepared using two different methods, elimination of microwave radiation is associated with the conducting and dielectrically lossy nature of MWCNTs.

2.6. Underlying Microwave Shielding Mechanism: A Large Dielectric Loss. To understand the mechanism behind microwave shielding in PC/PMMA blends, a closer look was taken on the complex dielectric properties over X and K_u-band frequencies. Figure 10 shows real and imaginary permittivity of PC/PMMA blends. Real permittivity (ε') corresponds to the storage of electrical energy and is greatly controlled by the polarization in the material. In this case, the polarization arises because of interfacial polarization induced by the large difference between the conductivities of the insulating polymer matrix and the conducting MWCNTs as well as from self-polarization associated with defective MWCNTs. Moreover, because of phase-separated blend structure and the selective localization of MWCNTs in the PC component, heterogeneous media were developed, which act as an interface for charge accumulation in the blends. The effect of blend composition (i.e., blend morphologies) on ε' is well-evident in both blend series. However, there is no direct relation between ε' and SE_T. Imaginary permittivity (ε'') represents the dielectric loss in the material and greatly controls the attenuation of microwave radiation. In this case, ε'' mainly corresponds to the Ohmic loss arising from nomadic charge transport through interconnected networks of MWCNTs. The ε'' was in line with the SE_T and SE_A observed in PC/PMMA blends. It is worth to note that the DC electrical conductivity of blends is not in line with ε'' observed in gigahertz frequencies for PC/PMMA blends. Hence, as mentioned earlier, the multiple intertube and interphase scattering has a great impact on dielectric loss and attenuation of microwave radiation. This is mainly due to enhanced interaction of penetrated microwave radiation with a large number of discrete MWCNTs in the conducting PC component. Therefore, it can be concluded that the observed absorption of microwave radiation was initiated by a large dielectric loss. For instance, in the case of solution-mixed 30/70 blends, the cocontinuous phase morphology and well-connected networks of MWCNTs led to maximum ε'', which is also confirmed by the highest SE_T and SE_A.

Figure 11a,b illustrates the role of multiple scattering and provides a possible mechanism of microwave attenuation in PC/PMMA blends. Hence, one can conclude that by developing heterogeneous media through selective localization of conducting nanoparticles (in this case MWCNTs) in immiscible polymer blends with cocontinuous phase structure and enhanced dispersion of nanoparticles by proper selection of processing methodology, enhanced multiple scattering can be

DOI: 10.1021/acsomega.8b00575
ACS Omega 2018, 3, 5771−5782

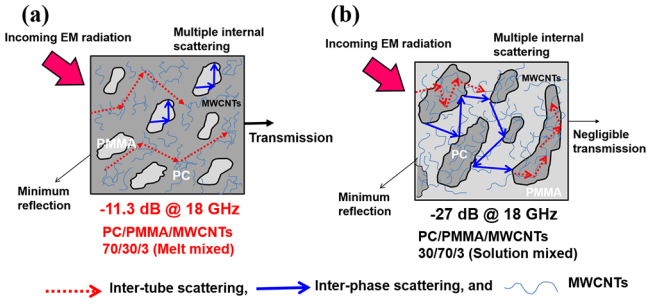

Figure 11. Cartoon illustrating the description of mechanism of microwave attenuation in (a) melt-mixed 70/30 and (b) solution-mixed 30/70 PC/PMMA blends containing 3 wt % MWCNTs.

achieved, which further facilitates enhanced elimination of incoming microwave radiation.

3. CONCLUSIONS

The effect of two traditional polymer blend nanocomposite fabrication processes on the development of blend microstructures, the quality of dispersion of MWCNTs, and the perfectness of migration into the thermodynamically preferred component was investigated in detail for various PC/PMMA blends containing MWCNTs using TEM analysis. In PC/PMMA blends prepared by solution or melt mixing, sea-island, cocontinuous, and phase-inverted microstructures can be obtained, depending on the blend composition. A significant effect of processing methodology on phase morphology was realized from TEM micrographs where melt-mixed blends depicted cocontinuous phase structure starting at 50 wt % of the PC component, whereas solution-mixed blends showed such morphologies already at 30 wt % of PC. In the latter case, the blends were mixed in the miscible state and phase separation occurred afterward during annealing above the glass-transition temperature of the components. Under these conditions, phase separation was restricted, which was also promoted by the additional influence of the nanotubes. Irrespective of the processing technique and blend composition, all blends showed selective localization of MWCNTs in the PC component. However, the perfectness of migration into this component depended on the PC content and its domain type and size on the blend preparation technique. It was better in melt-mixed than in solution-processed blends and was as high as the PC content. In solution-mixed blends, larger extended network structures not fitting into the PC component combined with longer nanotubes were observed. The state of dispersion was better in melt-mixed samples and if a higher accommodating PC volume was available. In solution-mixed blends with 3 wt % MWCNTs, in spite of similar electrical conductivities, a remarkable difference in EMI shielding performance of the blends was observed depending on their composition and blend microstructures. This implies that intertube and interphase scattering plays a vital role in the elimination of incoming microwave radiation. The highest EMI SE of −27 dB (@18 GHz), mainly through absorption, was achieved in PC/PMMA 30/70 solution-mixed blends containing 3 wt % MWCNTs. These blends were cocontinuous, with a relatively fine blend structure, showed in context with the low PC content a comparatively low degree of perfectness of nanotube migration, and had relatively long nanotubes so that quite large but segregated networks span over the sample volume. In summary, this study provides first critical insights on the effect of blend fabrication processes on the blend morphology, the nanotube arrangement, and the quality of dispersion of MWCNTs, resulting in different connectivities of the nanotube networks toward designing of high-performance microwave absorbers.

4. EXPERIMENTAL SECTION

4.1. Materials. For designing polymer blends, medium-viscosity PC Lexan 143R, Sabic and PMMA, Altuglas V825T, GSFC, India, were used. MWCNTs (NC 7000) from Nanocyl S.A., Sambreville, Belgium, with an average diameter of 9.5 nm and a length of 1.5 μm were used as conducting fillers.

4.2. Preparation of Nanocomposites. Melt mixing of the polymers and MWCNTs was carried out using a twin-screw HAAKE MiniLab II microcompounder with a set housing temperature of 260 °C and counter-rotating screw speed of 60 rpm for 20 min. To avoid oxidative degradation, melt mixing was performed under continuous flow of nitrogen. The blend components were vacuum-dried at 80 °C for 12 h to eliminate traces of moisture. All components were premixed and added together into the running compounder.

Solution mixing of PC/PMMA blends in tetrahydrofuran was done using bath sonication with a set power of 150 W for 30 min, followed by shear mixing using an Ultra-Turrax T25 shear mixer at 8000 rpm for 45 min. The nanocomposite was precipitated out using methanol and vacuum-dried to remove traces of solvent. After drying, the blend samples were then compression-molded at 260 °C for 20 min under 10 bar pressure.

4.3. Nanocomposite Characterization. *4.3.1. Morphology—OM and TEM.* Blend morphologies as well as selective localization and dispersion quality of MWCNTs in the blends were analyzed using OM and TEM. For OM, thin sections of 1 μm thickness were prepared from the solution-mixed and afterward compression-molded films using a Leica ultramicrotome and observed in transmission mode using an Olympus BX53M microscope combined with the Olympus camera DP71. For TEM investigations, a Zeiss Libra 120 microscope was used and the micrographs were captured with an accelerating voltage of 120 kV. In the case of melt-processed blends, ultrathin sections (thickness 60 nm) were cut from extruded strands using a microtome (Leica EM UC7) equipped with a diamond knife at a cutting speed of 0.4 mm/s at room temperature. For solution-mixed blends, 60 nm thin sections were cut from the compression-molded plates. No additional staining was done on the samples prior to the TEM imaging.

4.4. Electrical Volume Conductivity. For electrical measurements, PC/PMMA blends were compression-molded in a plate shape at 260 °C for 10 min. The measurements of electrical volume resistivity (ρ) of the nanocomposites were performed using a four-point test fixture (outer gold electrodes 16 mm distance, inner gold electrodes 10 mm) coupled with a Keithley E6517A or DMM 2000 electrometer at 25 °C and 45% relative humidity. The samples were cut from the pressed plates and had dimensions of 30 mm length and 3 mm width. Electrical volume conductivity (σ) was calculated from four measurements as a reciprocal of the obtained resistivity

$$\sigma = \frac{1}{\rho}$$

4.5. EMI Shielding. A vector network analyzer (VNA, Anritsu MS4642A) coupled with a Damaskos M07T coax setup

DOI: 10.1021/acsomega.8b00575
ACS Omega 2018, 3, 5771−5782

was employed to study the EMI shielding properties of the prepared nanocomposites. The reflection and absorption loss arising from the measurement set up and transmission lines was counterbalanced by complete two port short-open-load-through calibration prior to the measurements. The toroidal shape specimens with an outer and inner diameter of 7.00 and 3.04 mm, respectively, were compression-molded at 260 °C, and various scattering parameters were recorded over X and K_u-band frequencies. Complex permittivity values of nanocomposites were estimated using the Nicolson−Ross algorithm coupled with VNA.

■ ASSOCIATED CONTENT

Supporting Information

The Supporting Information is available free of charge on the ACS Publications website at DOI: 10.1021/acsomega.8b00575.

DSC thermographs of solution- and melt-mixed PC/PMMA (50/50) blends containing 3 wt % MWCNTs (PDF)

■ AUTHOR INFORMATION

Corresponding Authors

*E-mail: poe@ipfdd.de (P.P.).
*E-mail: sbose@iisc.ac.in (S.B.).

ORCID

Petra Pötschke: 0000-0001-6392-7880
Suryasarathi Bose: 0000-0001-8043-9192

Present Address

§Department of Chemical and Petroleum Engineering, University of Calgary, 2500 University Dr NW, Calgary, Canada, AB T2N 1N4.

Notes

The authors declare no competing financial interest.

■ ACKNOWLEDGMENTS

S.B., P.P., and S.P.P. would like to thank the Department of Science and Technology (DST)—German Academic Exchange Service (DAAD) for funding. In addition, S.B. would like to thank INSA (India) for the financial assistance. The authors would like to thank Manuela Heber (IPF Dresden) for assistance in TEM.

■ REFERENCES

(1) Tong, X. C. Electromagnetic Interference Shielding Fundamentals and Design Guide. *Advanced Materials and Design for Electromagnetic Interference Shielding*; CRC Press, 2016; pp 1−35.
(2) Qin, F.; Brosseau, C. A Review and Analysis of Microwave Absorption in Polymer Composites Filled with Carbonaceous Particles. *J. Appl. Phys.* **2012**, *111*, 061301.
(3) Li, Y.; Zhou, B.; Zheng, G.; Liu, X.; Li, T.; Yan, C.; Cheng, C.; Dai, K.; Liu, C.; Shen, C.; Guo, Z. Continuously Prepared Highly Conductive and Stretchable SWNT/MWNT Synergistically Composited Electrospun Thermoplastic Polyurethane Yarns for Wearable Sensing. *J. Mater. Chem. C* **2018**, *6*, 2258−2269.
(4) Wu, Z.; Gao, S.; Chen, L.; Jiang, D.; Shao, Q.; Zhang, B.; Zhai, Z.; Wang, C.; Zhao, M.; Ma, Y. Electrically Insulated Epoxy Nanocomposites Reinforced with Synergistic Core−Shell SiO_2@MWCNTs and Montmorillonite Bifillers. *Macromol. Chem. Phys.* **2017**, *218*, 1700357.
(5) Sun, K.; Xie, P.; Wang, Z.; Su, T.; Shao, Q.; Ryu, J.; Zhang, X.; Guo, J.; Shankar, A.; Li, J. Flexible Polydimethylsiloxane/Multi-Walled Carbon Nanotubes Membranous Metacomposites with Negative Permittivity. *Polymer* **2017**, *125*, 50−57.
(6) Pawar, S. P.; Biswas, S.; Kar, G. P.; Bose, S. High Frequency Millimetre Wave Absorbers Derived from Polymeric Nanocomposites. *Polymer* **2016**, *84*, 398−419.
(7) Geetha, S.; Satheesh Kumar, K. K.; Rao, C. R. K.; Vijayan, M.; Trivedi, D. C. EMI Shielding: Methods and Materials—a Review. *J. Appl. Polym. Sci.* **2009**, *112*, 2073−2086.
(8) Zhang, K.; Li, G.-H.; Feng, L.-M.; Wang, N.; Guo, J.; Sun, K.; Yu, K.-X.; Zeng, J.-B.; Li, T.; Guo, Z. Ultralow Percolation Threshold and Enhanced Electromagnetic Interference Shielding in Poly(L-Lactide)/Multi-Walled Carbon Nanotube Nanocomposites with Electrically Conductive Segregated Networks. *J. Mater. Chem. C* **2017**, *5*, 9359−9369.
(9) Liu, Z.; Bai, G.; Huang, Y.; Li, F.; Ma, Y.; Guo, T.; He, X.; Lin, X.; Gao, H.; Chen, Y. Microwave Absorption of Single-Walled Carbon Nanotubes/Soluble Cross-Linked Polyurethane Composites. *J. Phys. Chem. C* **2007**, *111*, 13696−13700.
(10) Pande, S.; Singh, B. P.; Mathur, R. B.; Dhami, T. L.; Saini, P.; Dhawan, S. K. Improved Electromagnetic Interference Shielding Properties of MWCNT−PMMA Composites Using Layered Structures. *Nanoscale Res. Lett.* **2009**, *4*, 327.
(11) Joo, J.; Lee, C. Y. High Frequency Electromagnetic Interference Shielding Response of Mixtures and Multilayer Films Based on Conducting Polymers. *J. Appl. Phys.* **2000**, *88*, 513−518.
(12) Bhattacharjee, Y.; Bhingardive, V.; Biswas, S.; Bose, S. Construction of a Carbon Fiber Based Layer-by-Layer (LbL) Assembly−a Smart Approach Towards Effective EMI Shielding. *RSC Adv.* **2016**, *6*, 112614−112619.
(13) Wang, Z.; Wei, R.; Liu, X. Fluffy and Ordered Graphene Multilayer Films with Improved Electromagnetic Interference Shielding over X-Band. *ACS Appl. Mater. Interfaces* **2017**, *9*, 22408−22419.
(14) Zhang, H.-B.; Yan, Q.; Zheng, W.-G.; He, Z.; Yu, Z.-Z. Tough Graphene−Polymer Microcellular Foams for Electromagnetic Interference Shielding. *ACS Appl. Mater. Interfaces* **2011**, *3*, 918−924.
(15) Yang, Y.; Gupta, M. C.; Dudley, K. L.; Lawrence, R. W. Novel Carbon Nanotube−Polystyrene Foam Composites for Electromagnetic Interference Shielding. *Nano Lett.* **2005**, *5*, 2131−2134.
(16) Eswaraiah, V.; Sankaranarayanan, V.; Ramaprabhu, S. Functionalized Graphene−PVDF Foam Composites for EMI Shielding. *Macromol. Mater. Eng.* **2011**, *296*, 894−898.
(17) Thomassin, J.-M.; Pagnoulle, C.; Bednarz, L.; Huynen, I.; Jerome, R.; Detrembleur, C. Foams of Polycaprolactone/MWNT Nanocomposites for Efficient EMI Reduction. *J. Mater. Chem.* **2008**, *18*, 792−796.
(18) Wang, Z.; Jia, K.; Liu, X. Temperature Dependent Electrical Conductivity and Microwave Absorption Properties of Composites Based on Multi-Wall Carbon Nanotubes and Phthalocyanine Polymer. *J. Mater. Sci. Mater. Electron.* **2015**, *26*, 8008−8016.
(19) Chung, D. D. L. Electromagnetic Interference Shielding Effectiveness of Carbon Materials. *Carbon* **2001**, *39*, 279−285.
(20) Ma, P. C.; Kim, J.-K.; Tang, B. Z. Effects of Silane Functionalization on the Properties of Carbon Nanotube/Epoxy Nanocomposites. *Compos. Sci. Technol.* **2007**, *67*, 2965−2972.
(21) Ma, P.-C.; Mo, S.-Y.; Tang, B.-Z.; Kim, J.-K. Dispersion, Interfacial Interaction and Re-Agglomeration of Functionalized Carbon Nanotubes in Epoxy Composites. *Carbon* **2010**, *48*, 1824−1834.
(22) Ma, P.-C.; Siddiqui, N. A.; Marom, G.; Kim, J.-K. Dispersion and Functionalization of Carbon Nanotubes for Polymer-Based Nanocomposites: A Review. *Composites, Part A* **2010**, *41*, 1345−1367.
(23) Pawar, S. P.; Gandi, M.; Saraf, C.; Bose, S. Exceptional Microwave Absorption in Soft Polymeric Nanocomposites Facilitated by Engineered Nanostructures. *J. Mater. Chem. C* **2016**, *4*, 4954−4966.
(24) Pawar, S. P.; Gandi, M.; Bose, S. High Performance Electromagnetic Wave Absorbers Derived from PC/SAN Blends Containing Multiwall Carbon Nanotubes and Fe_3O_4 Decorated onto Graphene Oxide Sheets. *RSC Adv.* **2016**, *6*, 37633−37645.
(25) Pawar, S. P.; Marathe, D. A.; Pattabhi, K.; Bose, S. Electromagnetic Interference Shielding through MWNT Grafted

DOI: 10.1021/acsomega.8b00575
ACS Omega 2018, 3, 5771−5782

Fe_3O_4 Nanoparticles in PC/SAN Blends. *J. Mater. Chem. A* **2015**, *3*, 656−669.
(26) Zeraati, A. S.; Arjmand, M.; Sundararaj, U. Silver Nanowire/MnO_2 Nanowire Hybrid Polymer Nanocomposites: Materials with High Dielectric Permittivity and Low Dielectric Loss. *ACS Appl. Mater. Interfaces* **2017**, *9*, 14328−14336.
(27) Li, Y.; Shimizu, H. Conductive PVDF/PA6/CNTs Nanocomposites Fabricated by Dual Formation of Cocontinuous and Nanodispersion Structures. *Macromolecules* **2008**, *41*, 5339−5344.
(28) Göldel, A.; Kasaliwal, G.; Pötschke, P. Selective Localization and Migration of Multiwalled Carbon Nanotubes in Blends of Polycarbonate and Poly(Styrene-Acrylonitrile). *Macromol. Rapid Commun.* **2009**, *30*, 423−429.
(29) Bose, S.; Bhattacharyya, A. R.; Kulkarni, A. R.; Pötschke, P. Electrical, Rheological and Morphological Studies in Co-Continuous Blends of Polyamide 6 and Acrylonitrile−Butadiene−Styrene with Multiwall Carbon Nanotubes Prepared by Melt Blending. *Compos. Sci. Technol.* **2009**, *69*, 365−372.
(30) Pawar, S. P.; Gandi, M.; Arief, I.; Krause, B.; Pötschke, P.; Bose, S. Graphene Derivatives Doped with Nickel Ferrite Nanoparticles as Excellent Microwave Absorbers in Soft Nanocomposites. *ChemistrySelect* **2017**, *2*, 5984−5999.
(31) Zhao, X.; Zhao, J.; Cao, J.-P.; Wang, D.; Hu, G.-H.; Chen, F.; Dang, Z.-M. Effect of the Selective Localization of Carbon Nanotubes in Polystyrene/Poly(Vinylidene Fluoride) Blends on Their Dielectric, Thermal, and Mechanical Properties. *Mater. Des.* **2014**, *56*, 807−815.
(32) Pötschke, P.; Pegel, S.; Claes, M.; Bonduel, D. A Novel Strategy to Incorporate Carbon Nanotubes into Thermoplastic Matrices. *Macromol. Rapid Commun.* **2008**, *29*, 244−251.
(33) Miles, I. S.; Zurek, A. Preparation, Structure, and Properties of Two-Phase Co-Continuous Polymer Blends. *Polym. Eng. Sci.* **1988**, *28*, 796−805.
(34) Steinmann, S.; Gronski, W.; Friedrich, C. Cocontinuous Polymer Blends: Influence of Viscosity and Elasticity Ratios of the Constituent Polymers on Phase Inversion. *Polymer* **2001**, *42*, 6619−6629.
(35) Bae, D.-Y.; Lee, H.-S. Enhanced Compatibility of PC/PMMA Alloys by Adding Multiwall Carbon Nanotubes. *Carbon Lett.* **2010**, *11*, 83−89.
(36) Liebscher, M.; Tzounis, L.; Pötschke, P.; Heinrich, G. Influence of the Viscosity Ratio in PC/SAN Blends Filled with MWCNTs on the Morphological, Electrical, and Melt Rheological Properties. *Polymer* **2013**, *54*, 6801−6808.
(37) Marin, N.; Favis, B. D. Co-Continuous Morphology Development in Partially Miscible PMMA/PC Blends. *Polymer* **2002**, *43*, 4723−4731.
(38) Chiou, J. S.; Barlow, J. W.; Paul, D. R. Miscibility of Bisphenol-a Polycarbonate with Poly(Methyl Methacrylate). *J. Polym. Sci., Part B: Polym. Phys.* **1987**, *25*, 1459−1471.
(39) Nishimoto, M.; Keskkula, H.; Paul, D. R. Role of Slow Phase Separation in Assessing the Equilibrium Phase Behaviour of PC-PMMA Blends. *Polymer* **1991**, *32*, 272−278.
(40) Gültner, M.; Göldel, A.; Pötschke, P. Tuning the Localization of Functionalized MWCNTs in SAN/PC Blends by a Reactive Component. *Compos. Sci. Technol.* **2011**, *72*, 41−48.
(41) Pötschke, P.; Bhattacharyya, A. R.; Janke, A. Morphology and Electrical Resistivity of Melt Mixed Blends of Polyethylene and Carbon Nanotube Filled Polycarbonate. *Polymer* **2003**, *44*, 8061−8069.
(42) Bose, S.; Bhattacharyya, A. R.; Bondre, A. P.; Kulkarni, A. R.; Pötschke, P. Rheology, Electrical Conductivity, and the Phase Behavior of Cocontinuous PA6/ABS Blends with MWNT: Correlating the Aspect Ratio of MWNT with the Percolation Threshold. *J. Polym. Sci., Part B: Polym. Phys.* **2008**, *46*, 1619−1631.
(43) Pötschke, P.; Bhattacharyya, A. R.; Janke, A. Carbon Nanotube-Filled Polycarbonate Composites Produced by Melt Mixing and Their Use in Blends with Polyethylene. *Carbon* **2004**, *42*, 965−969.
(44) Pawar, S. P.; Bose, S. Peculiar Morphological Transitions Induced by Nanoparticles in Polymeric Blends: Retarded Relaxation or Altered Interfacial Tension? *Phys. Chem. Chem. Phys.* **2015**, *17*, 14470−14478.
(45) Park, J.; Lee, S.; Lee, J. W. Effect of Manufacturing Condition in PC/PMMA/CNT Nanocomposites Extrusion on the Electrical, Morphological, and Mechanical Properties. *Korea Aust. Rheol. J.* **2015**, *27*, 55−62.
(46) Krause, B.; Villmow, T.; Boldt, R.; Mende, M.; Petzold, G.; Pötschke, P. Influence of Dry Grinding in a Ball Mill on the Length of Multiwalled Carbon Nanotubes and Their Dispersion and Percolation Behaviour in Melt Mixed Polycarbonate Composites. *Compos. Sci. Technol.* **2011**, *71*, 1145−1153.
(47) Pötschke, P.; Villmow, T.; Krause, B. Melt Mixed PCL/MWCNT Composites Prepared at Different Rotation Speeds: Characterization of Rheological, Thermal, and Electrical Properties, Molecular Weight, MWCNT Macrodispersion, and MWCNT Length Distribution. *Polymer* **2013**, *54*, 3071−3078.
(48) Talò, M.; Krause, B.; Pionteck, J.; Lanzara, G.; Lacarbonara, W. An Updated Micromechanical Model Based on Morphological Characterization of Carbon Nanotube Nanocomposites. *Composites, Part B* **2017**, *115*, 70−78.
(49) Krause, B.; Mende, M.; Petzold, G.; Boldt, R.; Pötschke, P. Characterization of Dispersability of Industrial Nanotube Materials and Their Length Distribution before and after Melt Processing. In *Carbon Nanotube−Polymer Composites*; Tasis, D., Ed.; Royal Society of Chemistry: Cambridge, U.K., 2013; p 212.
(50) Krause, B.; Boldt, R.; Pötschke, P. A Method for Determination of Length Distributions of Multiwalled Carbon Nanotubes before and after Melt Processing. *Carbon* **2011**, *49*, 1243−1247.
(51) Liebscher, M.; Domurath, J.; Krause, B.; Saphiannikova, M.; Heinrich, G.; Pötschke, P. Electrical and Melt Rheological Characterization of PC and Co-Continuous PC/SAN Blends Filled with CNTs: Relationship between Melt-Mixing Parameters, Filler Dispersion, and Filler Aspect Ratio. *J. Polym. Sci., Part B: Polym. Phys.* **2018**, *56*, 79−88.
(52) Faraguna, F.; Pötschke, P.; Pionteck, J. Preparation of Polystyrene Nanocomposites with Functionalized Carbon Nanotubes by Melt and Solution Mixing: Investigation of Dispersion, Melt Rheology, Electrical and Thermal Properties. *Polymer* **2017**, *132*, 325−341.

DOI: 10.1021/acsomega.8b00575
ACS Omega 2018, 3, 5771−5782